HIGH RESOLUTION SST MAPPING USING AVHRR-CALIBRATED TM DATA

J.A.Triñanes,A.Tobar,*C.Bóveda,C.Hernández.

Department of Applied Physics. Faculty of Physics. University of Santiago.Spain.

*Department of Computer Sciencies. Faculty of Informatics. University of Coruña.Spain.

RÉSUMÉ

Nous présentons ici una méthode pour réaliser cartes thermiques marines d'haute resolution (120 mx120m) en combinant des données des satellites NOAA and Landsat. Nous employons l'algorithme *split-window* pour calculer la carte thermique de la surface marine (SST) des données du NOAA. Nous corrélons cette carte thermique NOAA avec la bande six du Landsat. Nous selectionnons des points geographiques, pour obtenir pairs (TM,SST), en utilisant trois méthodes. Les coefficients de regression calculés pour les trois méthodes furent très semblables et assignent la même temperature aux valeurs numerisées de la bande six du Landsat. Nos resultats coincident avec les obtenu pour Anuta et collaborateurs. En utilisant la valeur du coefficient de regression obtenu por Anuta, nous calculons la curve de calibration.

ABSTRACT

The multispectral capabilities of the AVHRR sensors on the most recent NOAA satellites allow high-precision calculation of sea surface temperature (SSTs), but the spatial resolution of these data is insufficient for studies of many phenomena of interest in coastal zones (e.g. movements of pelagic species, sedimentation dynamics, red tides, and the evolution of pollutant plumes). Band 6 of the Landsat 5 TM sensor, on the other hand, has good spatial resolution (120 x 120 m per pixel) but, as a single band, does not afford SSTs. In this work we used AVHRR SST data to calibrate the TM Band 6 radiance data for high-resolution SST mapping of the coastal waters of Galicia (N.W. Spain).

INTRODUCTION

The marine remote sensing technique which has had the greatest impact on oceanography is that of the monitoring of sea surface temperatures (SST) by radiometers fitted to Earth orbiting satellites. However, for nearly ten years, until Landsat-4 began to operate, satellite users did not have access to high spatial resolution IR thermal data.

Temperatures measured from space are obviously surface temperatures and their usefulness in oceanography depends on our ability to interpret them in relation to underlying temperatures in lower layers of the ocean (down to a depth of a few metres).

The exact determination of sea surface temperature is essential in oceanic and climatic studies. The thermal structure of the ocean plays a critical role in the regulation of interchange systems between the atmosphere and water masses, and a knowledge of ocean surface temperatures in essential for the verification of circulation models. Prospecting for marine resources, studies of the marine environment and the understanding of dynamic phenomena in coastal waters [7],[12],[13] and estuaries are other fields which will benefit greatly in their development from the measurement of sea surface temperatures by satellite sensors.

OBJECTIVES

Our objective is to take advantage of the high spatial resolution of the TM sensor and the precise thermal measurements from NOAA in order to obtain extremely accurate temperature maps of the coast of Galicia (NW Spain) far superior to any yet available, and which would be applicable to any other region at a much lower cost (in terms of both time and money) than that involved in a similar study carried out using conventional methods of temperature measurement of the surface layers of the sea.

The evaluation of results takes into account a study completed by a research group at Purdue University headed by Paul E. Anuta [1] which provides extensive analysis of the characteristics of Landsat images and, more specifically, a concise study with reference to Band 6 of the TM sensor. Anuta et al. attempted to transform the relative responses to IR thermal (or rather their digital levels) into radiant temperatures. This process requires the use of a non-linear calibration function specifically derived for the thermal TM band and the temperature scale of the two internal black bodies.

TEST DATA SETS

The Landsat TM image with which we worked corresponds to the 205th orbit, row 30, fourth quadrant of an image received by the Fucino Satellite Station in Italy on August 18th 1991.

For the NOAA images we have access to an image receiver for NOAA-9, -10, -11 and -12. This provides extensive and constantly up-dated information on phenomena which, potentially, can be observed by these satellites. Among these phenomena is the measurement of sea surface temperatures which forms the basis of

our research. The AVHRR data were obtained in real time from NOAA-11 on August 19th 1991.

IMAGES PREPROCESSING

Before comparing both images the area for study had to be delimited. To take maximum advantage of the surface area to be studied we isolated the area on the Landsat image containing the greatest number of pixels associated with water masses. In this way an extract of 1837 columns and 1921 rows was obtained within which the estuaries of Noya and Arosa and the upper reaches of the estuary of Pontevedra can be clearly appreciated.

The only band of the TM sensor which is of interest in this particular field of research is the thermal band (Band 6) and, consequently, it was necessary to separate it from the other bands which go to make up the image. When the pixels corresponding to the sea are enhanced an effect characteristic to Landsat images - *striping* - is observed. This is the result of bad calibration between the various sensors that constitute the sensor unit - that is to say that some of the sensors codify the radiance that they receive with inferior or superior digital levels to the rest. What is more, the sensor memory emphasizes this effect when the sensor passes from zones of high reflectance to zones of low reflectance.

Due to the fact that the resolution of the thermal band is four times greater than that of the other bands each sample is represented by a group of 4x4 pixels. A detailed analysis of the image reveals that one in every ten lines of the sample group deviates from the preceding line and that within that portion the sample is formed by groups of 4x5 pixels. The reason for this deviation could be a mal-function in the multiplex responsible for codifying and formatting the data received by the TM sensor detectors or an error in one of the algorithms employed by the satellite image receiver station to correct the effect of panoramic distortion, terrestrial rotation, the speed of the mirror sweep, etc.

We tried various methods in order to eliminate the effect of this *noise* on the image, among them the equalization of histograms for each detector in the sensor unit [4], the transformation of the image in terms of its spatial frequency components (using Fourier's transformed)[3],[6],[8] and, finally, the application of filters in the spatial domain [11].

Within the surface area under investigation the DL (Digital Levels) variations between adjacent samples do not exceed 2 units. This small, local variation between pixels suggests the need for the use of a process of image smoothing using a mobile matrix with filtering coefficients. This matrix, also denominated kernel, can vary in size depending on the number of adjacent pixels we wish to study in the process. After using various types of filters we reached the conclusion that the best suited to our needs was the median filter [11]. This offers a series of advantages that make it particularly useful; the median of a group of n numbers in always equal to one of the values present within that same group; the median is much less sensitive to errors or to extreme values within the data. This is why the median filter preserves the contours better than other filters which smooths the grey content around the central pixel in the filter window.

First the data received from NOAA-11 must be retrieved from the lines which have been disturbed during the process of transmission, either being lost or changing the pixel values which go to make up the image.

The next step is to convert the digital values of the various bands to brightness temperatures [15] or % albedo. The calibration algorithm is based on information contained in [10]. Different tests are applied to the image to extract those areas covered by cloud or partially covered. The *split-window* algorithm [5],[7],[13]allows us to relate the radiant temperatures in channels 4 and 5 so that we can obtain an estimated sea surface temperature to within 0.1°C error.

$$SST = a\,T_4 + b(T_4 - T_5) + c$$

Both images have to be referenced with respect to the same coordinate system [2],[4],[11],[14]. More concisely, the Landsat image has to be rectified so that it can be superimposed on the NOAA-11 temperature map to enable us to identify training samples, extract their statistics and produce a regression line which relates the temperatures from one band with the digital levels of the other. This rectification is carried out using so-called control points. Taking into account the great difference in resolution between the two images (120 m. - 1.1 Km.) the obvious choise for these control points are the coastlines and, for this reason, the reference band in NOAA image is Band 3 which provides a much better differentiation of coastlines than the other bands of the AVHRR image sensor. A first order transformation is a linear transformation allowing us to scale, skew, rotate and shift. These characteristics are sufficient for our purposes. A total of 22 control points was chosen, a high number for the transformation order that was used for which 3 control points are sufficient. We have overcome this minimum value in order to guarantee a reasonable degree of conformity between image and map. In addition the points are uniformly distributed along the coastline which avoids errors resulting from excessive weighting in any one sector of the study area. The Root Mean Square error (RMS error) for all the control points facilitates the evaluation of the general quality of the adjustment. If this value is not satisfactory we can opt for eliminating those points which have a high RMS error as it can be assumed that they have been incorrectly situated. When a control point is eliminated the adjustment function and the RMS error of each remaining point is calculated again. The process is interrupted when the chosen control points have an RMS error below a certain threshold which has been fixed at 10. As regards the rectification algorithm it has been shown that the nearest neighbour method, bilinear interpolation and cubic convolution all give the same results. We decided to keep to the first method as in terms of computation *cost* it is much *cheaper* than the other two.

CLASSIFICATION

A new file which contains the transformed Landsat thermal band and the band corresponding to the temperature map was created.

At this stage it was necessary to employ the various classification methods [16],[14] known to us: operator supervised methods, un-supervised or automatic methods and, finally, a

synthesis of these two types which should, theoretically, give optimum results.

For the supervised method a training area was chosen in which clustering was used, extracting statistics from different homogeneous groups and analysing them to create the regression line at which we have arrived.

For the automatic method the ISODATA [4] algorithm was used. Finally, a synthesis of these two methods was used which involves the supervised phase of training group selection to which the ISODATA algorithm was then applied. In order to calculate the statistical separability of the various groups both transformed divergence and Jeffries Matusita distance were used. The results produced values which indicate large separability between groups and, then, this confirms the clear discrimination of the different spectral signatures.

Given that the two satellite images do not correspond to the same day and that, therefore, some water masses have moved in relation to one another, which suggests the need to employ band by band classification (that is identifying homogeneous areas in both images and then relatin them statistically) the results thus obtained were very similar to those obtained using any of the formerly mentioned methods.

RESULTS

The final results are shown below:

	a0	a1(slope)
Supervised Classification	-8.7342392	0.2248968
Unsupervised Clasiffication	-8.8349213	0.2257660
Mixed Clasification	-8.1477783	0.2198829
Band by band	-9.7828743	0.2339363
Band by band (Not taking into account pixels situated near the limits between areas)	-9.9802620	0.2356284

As it can be appreciated from the regression lines which were reached both the slope and the constants were very similar which corroborates the reliability of the results obtained. In addition to this the correlation coefficient of each of the lines presents a value very close to a unit.

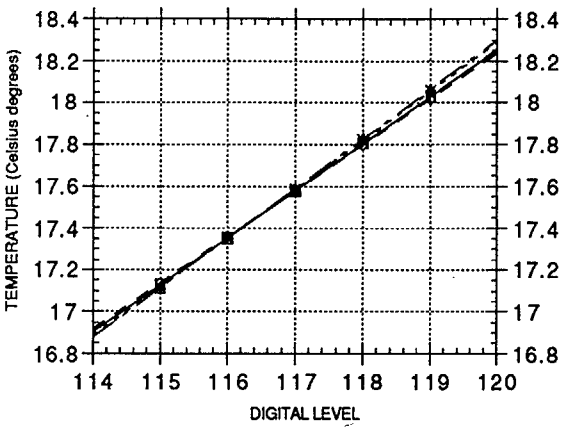

Figure 1. SST´s from regression lines versus TM digital levels.

A simple program allows us to apply the conversion line which we have reached to the data for the thermal Landsat TM. In this way a temperature map for the zone is obtained which has a spatial resolution far greater than any yet available.

At this point Anuta's estimated results are used. The equation at which they arrived can be used to approximate the digital levels present in the image (114-120) which creates a regression line represented by the following equation:

$$T\ (°C) = 0.2374109 - 9.491353 * DL$$

Taking into account that the TM sensor has a similar slope to that of the above equation and extrapolating the results we arrive at a regression line which can be used on the image:

$$T\ (°C) = 0.2374109 - 10.18755 * DL$$

The objective has been reached. Given a grey level in the thermal band of the Landsat images we can establish a temperature value associated to each pixel in the image to within an estimated error virtually identical to that of the AVHRR sensor simply by employing a simple equation.

CONCLUSIONS AND FUTURE RESEARCH TOPICS

This general procedure for the extraction of high resolution maps is based on the thermal channel of a TM image and the temperature map obtained using multispectral analysis of another AVHRR image which covers the same area and which has a minimal time separation with respect to the first. This can be of invaluable help in producing a thermal cartography of the coast, observing the seasonal evolution of the water masses, detecting phenomena such as upwelling and oceanic fronts (which has great importance for the fishing and sea food industries in the area) and, with the help of the other Thematic Mapper bands, studying the evolution of red tides, pollution focus both within and outside estuaries, the dynamics of sediment deposition, etc. All this will enable us to obtain a greater understanding of the marine dynamics at work on the Galician coast, which can be applied to any other geographical point on the Earth's surface without having to alter in any way the algorithm used.

It would be more convenient to have access to field measurements of SSTs but for the date of acquisition of the images they were unavailable. Further studies will allow us to calibrate the coefficients used in the split-window algorithm so that the temperature maps will be as accurate as possible and, consequently, the final results will be even more precise.

The process has been completely automated based on the correlation between both images using a window whose size is mxn [9] so the points with the highest correlation coefficient are chosen to be used. This method provides similar results to the above but the process is easier to automate and also quicker than that previously mentioned.

Finally, the field of synthesis of data from different remote sensors is thought to be one of the research fields with a great future given the increasing availability of imagery from different sources and its progressively decreasing price.

The next page image shows the results obtained.

References

1.- Anuta, Paul E. y colaboradores, "Landsat-4 MSS and Thematic Mapper Data Quality and Information Content Analysis", *IEEE Transactions on Geoscience and Remote Sensing*,vol.GE-22,no.3, May 1984.

2.- Bernstein, R., "Digital Image Processing of Earth Observation Sensor Data", *IBM J. Res. Develop.*, vol. 20, pp. 40-57,Jan. 1976.

3.- Castleman, Kenneth R., *Digital Image Processing*, Prentice-Hall, 1979.

4.- Chuvieco, Emilio, *Fundamentos de Teledetección Espacial*, Ediciones Rialp, 1990.

5.- Deepak, Adarsh, *Remote Sensing of Atmospheres and Oceans*, Academic Press, 1979.

6.- Gonzalez, Rafael C. y Wintz Paul, *Digital Image Processing*, Addison-Wesley Publishing Company, 1977.

7.- Gower, J.F.R., *Oceanography from Space*, Plenum Press, 1981.

8.- Hord, R. Michael, *Digital Image Procéssing of Remotely Sensed Data*, Academic Press, 1982.

9.- Hord, R. Michael, *Remote Sensing: Methods and Aplications*, Wiley-Interscience, 1986.

10.- Lauritson, Levin y Nelson, Gary, "Techniques for Data Extraction and Calibration of TIROS-N/NOAA Series Satellite Radiometers for Direct Readout Users", *NOAA-NESS Publication* #107, July 1979.

11.- Mather, Paul M., *Computer Processing of Remotely-Sensed Images*, John Wiley&Sons, 1987.

12.- Richards, Francis A., *Coastal Upwelling*, AGU, 1981.

13.- Saltzman, Barry, *Satellite Oceanic Remote Sensing*, Academic Press, 1985.

14.- Schowengerdt, Robert A., *Techniques for Image Processing and Classification in Remote Sensing*, Academic Press, 1983.

15.- Szekielda, Karl-Heinz, *Satellite Monitoring of the Earth*, Wiley Interscience, 1988.

16.- Townshend, J.R.G., *Terrain Analysis and Remote Sensing*, George Allen&Unwin, 1981.

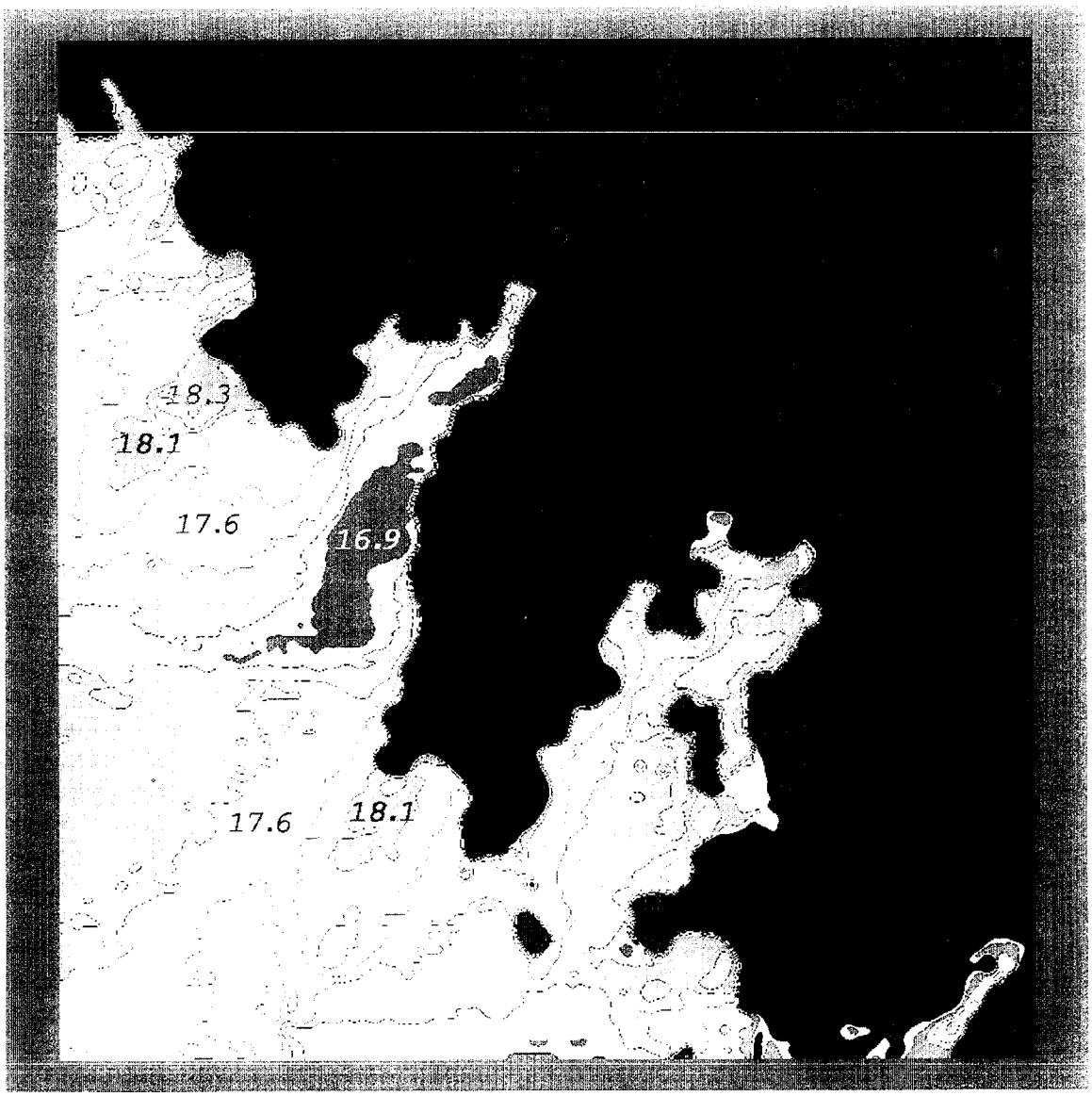

Figure 2. High resolution SST map